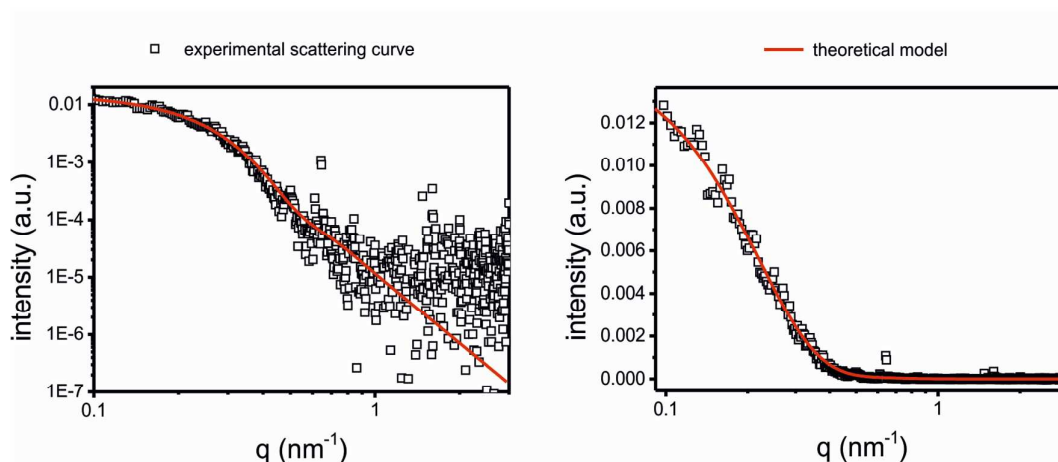


## Supporting Information

**All concentrations refer to the reactant solutions that are used to synthesize the colloidal nanoparticles! The reactant solutions are mixed 1:1 with the reducing agent solution or the silver precursor solution, respectively.**

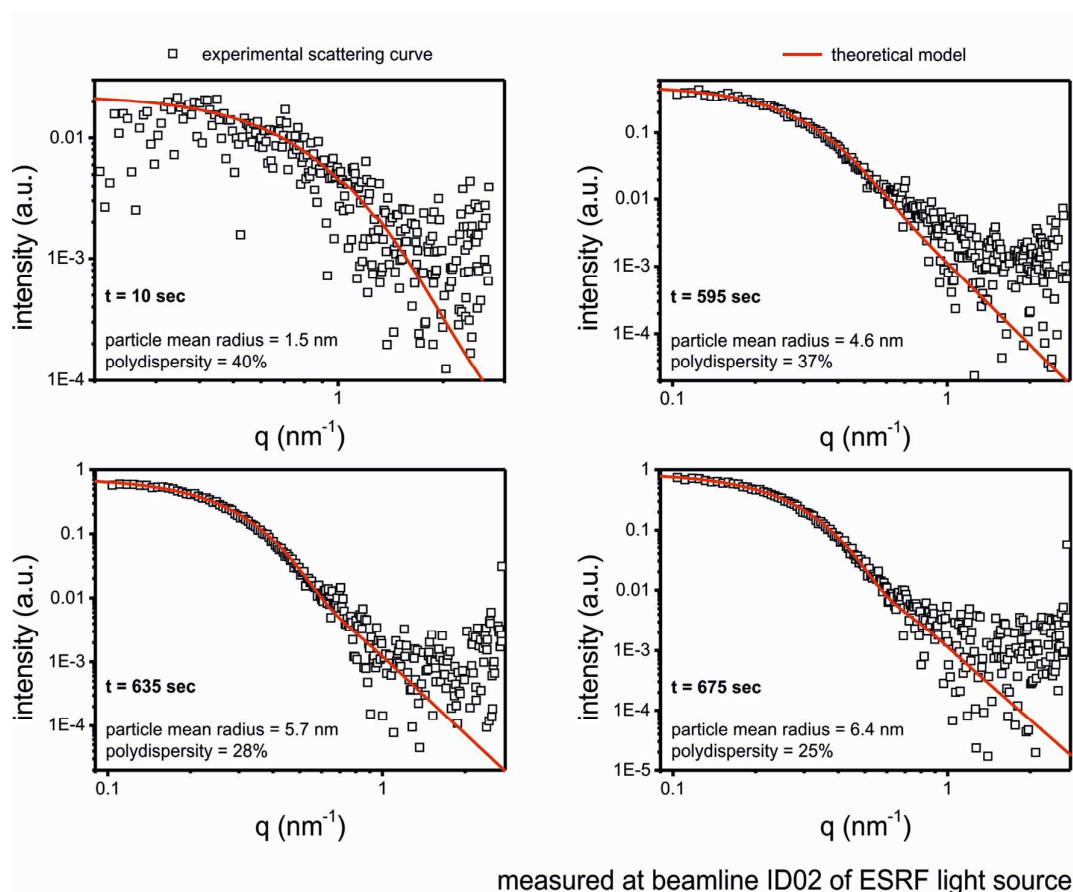
SAXS data derived from lab-scale experiments are in general noisier compared to data derived from synchrotron experiments. One reason is the desmearing process, a mathematical data treatment which becomes necessary when a slit focus is used instead of a point focus. However, the data quality derived by the lab-scale SAXS machine is sufficient to calculate the nanoparticle size distribution accurately. Below we displayed a selected scattering curve using a linear rather than a logarithmic y-scale. The figure illustrates that the scattering intensity for  $q > 0.7$  is almost zero. Therefore, the influence of the mathematical fit on the derived parameters (mean radius, polydispersity, and volume fraction) is negligible for this  $q$ -range.



Selected scattering curve and mathematical fit displayed in logarithmic and linear y-scale.

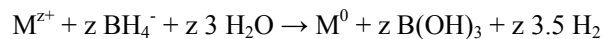
## SI-1

SAXS data from the time-resolved investigation of the principle growth mechanism: selected scattering curves and the corresponding fits for different reaction times.

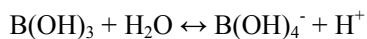


## SI-2

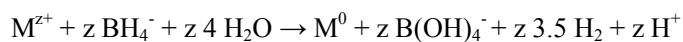
(i) The chemical reduction of a metal species  $M^{z+}$  by  $BH_4^-$  is a complex process. Glavée et al. studied the reaction for a variety of metal ions.<sup>1</sup> They determined the stoichiometric factors and deduced a balanced equation which can be expressed universally as



for metals M with a positive redox potential. Using Raman spectroscopy, Edwards and coworkers showed that boric acid  $B(OH)_3$  does not act as Brønsted acid in aqueous solution.<sup>2</sup> Instead, it serves as Lewis acid which leads to the formation of the tetrahydroxyborate anion:



Subsequently, the overall reaction equation can be expressed by:



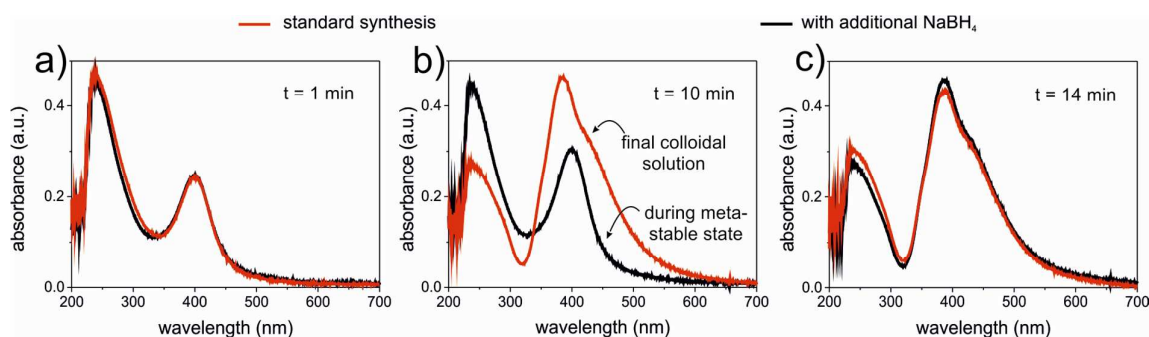
(ii) The reaction of  $BH_4^-$  with water (hydrolysis) has been studied for different conditions (concentration, temperature, pH value, with and without nanoparticles) by several groups.<sup>3-6</sup> For information on the reaction mechanism see Gonçalves *et al.*<sup>7</sup>

### SI-3

The duration of the metastable state can be extended by addition of  $\text{BH}_4^-$  after the first coalescence. This can be deduced from a simple experiment:

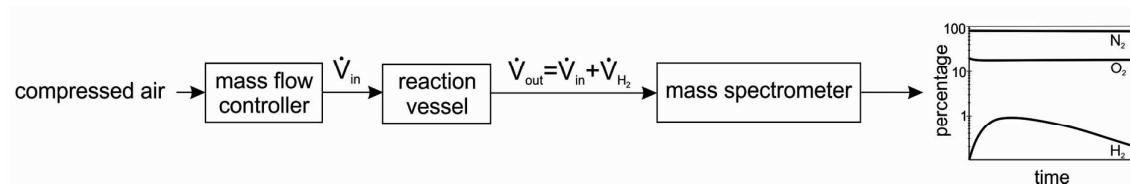
10 mL of a 3 mM  $\text{NaBH}_4$  solution and 10 mL of a 0.5 mM  $\text{AgClO}_4$  solution are mixed 1:1. After 10 sec, the solution is split into two equal parts. To one of the samples, 300  $\mu\text{L}$  of the  $\text{NaBH}_4$  solution are added. Every minute, the UV-vis spectra of each sample are recorded. The figure displays the spectra for 1, 10 and 14 min.

The plasmonic properties of silver nanoparticles are size dependent.<sup>8</sup> Therefore, the metastable phase and the final colloidal solution can be distinguished easily: The spectrum shows two absorption peaks at 237 and 401 nm during the metastable state while the final colloidal solution is characterized by absorption maxima at 237 and 383 nm.<sup>9</sup> The spectra of the samples collected at 1 min can both be ascribed to the metastable state. The spectrum of the standard sample collected at 10 min reveals that the last growth step (second coalescence) is finished and the final colloidal solution is already obtained. In contrast, the spectrum of the colloidal solution with additional  $\text{NaBH}_4$  can still be ascribed to the metastable state. The spectra for a reaction time of 14 min indicate for both solutions the final colloidal solution with a similar size distribution.

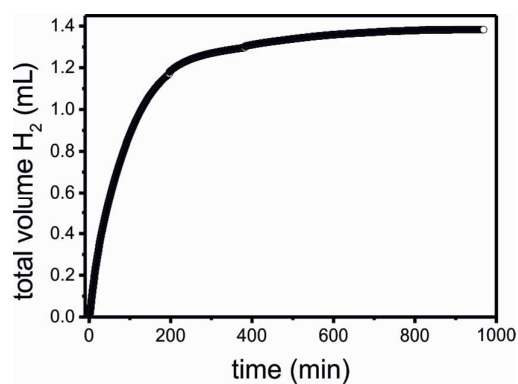


#### SI-4

a) The illustration shows the schematic setup for time-resolved hydrogen monitoring via MS spectrometry. A description can be found in the Experimental part.



b) The figure below depicts the total volume of released  $H_2$  vs. time for 10 mL of a 1.5 mM  $NaBH_4$  solution which was obtained by 1:1 mixing of water and the standard reducing agent solution.

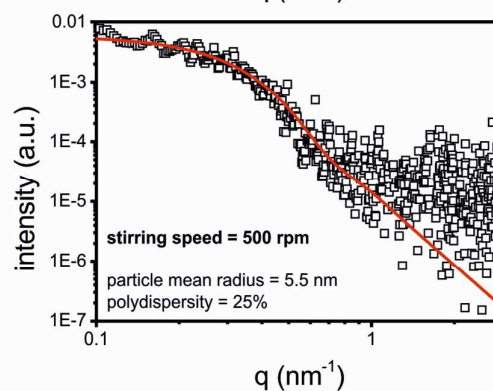
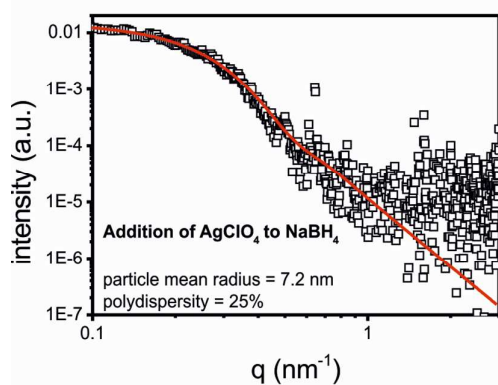
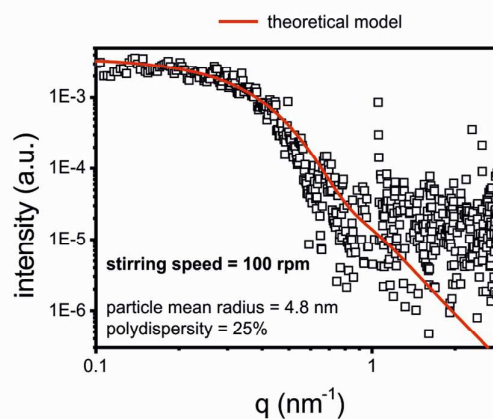
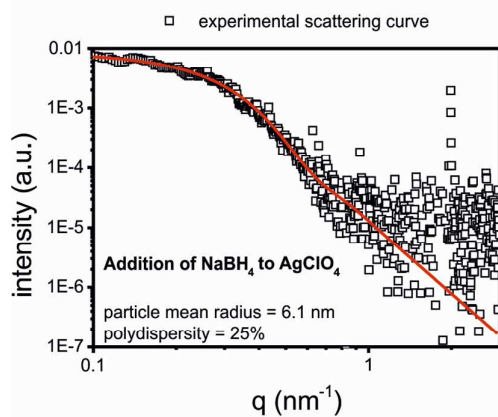


## SI-5

Almost any change of the procedure influences the nanoparticle synthesis. The table illustrates the influences of mixing conditions and stirring speed on the final size distribution (polydispersity is constantly 25%). The size distributions were determined by lab-scale SAXS. Selected scattering curves and corresponding mathematical fits are displayed below.

Mixing procedure	Final particle mean radius (nm)
1:1	5.9
	6.6
	4.4
Addition of $\text{AgClO}_4$ to $\text{NaBH}_4$	7.2
	7.4
	6.5
Addition of $\text{NaBH}_4$ to $\text{AgClO}_4$	6.1
	5.9
	6.7

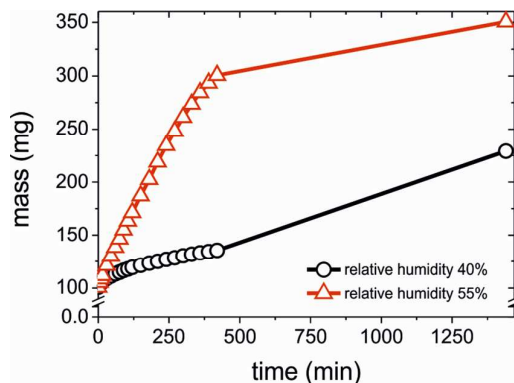
Stirring Speed (rpm)	Final particle mean radius (nm)
100	4.7
	4.9
	4.8
300	3.7
	4.8
	4.0
500	6.7
	5.5
	6.2



measured with lab-scale SAXS machine

## SI-6

$\text{NaBH}_4$  is a hygroscopic substance. The absorption of moisture can be illustrated by monitoring the mass increase of a sample which is stored unsealed/open. 100 mg  $\text{NaBH}_4$  powder were placed on a weighing dish and stored (unsealed) on a balance. The figure depicts the mass vs. time for a relative humidity of 40% and 55%, respectively. After 24 h, the solid is covered by a liquid film or even dissolved completely. The relative mass increases to 225% (humidity = 40%) and 350% (humidity = 55%), respectively.





## SI-7

To study the influence of the reactant concentrations, the  $\text{AgClO}_4$  concentration was varied between 0.25 and 0.75 mM and the  $\text{NaBH}_4$  concentration was varied between 1.5 and 4.5 mM. The final colloidal solutions were investigated with lab-scale SAXS. The scheme lists the average particle mean radii with the standard deviations of the three samples. In addition, the ratio of the reactant concentrations and the average duration of the metastable state (time until the colloidal solution turns from yellow to orange-brown) are displayed. Note: Since the amount of residual  $\text{BH}_4^-$  is not identical for identical ratios of  $[\text{NaBH}_4]/[\text{AgClO}_4]$  the duration of the metastable state differs.

The dark blue boxes highlight the results of the standard synthesis (displayed twice). The light blue boxes highlight syntheses for which the growth mechanism is investigated in a further parameter study (see Figure 3).

### Variation of the $\text{AgClO}_4$ concentration for $[\text{NaBH}_4] = 3 \text{ mM}$

a)	$[\text{AgClO}_4]$	0.25 mM	0.4 mM	0.5 mM	0.6 mM	0.75 mM
	mean radius	7.2 nm	9.0 nm	9.9 nm	10.0 nm	10.4 nm
	deviation of mean radius	0.3 nm	0.3 nm	0.6 nm	0.9 nm	0.7 nm
	duration of metastable state	804 sec	540 sec	437 sec	494 sec	400 sec
	$[\text{NaBH}_4]/[\text{AgClO}_4]$	12	7.5	6	5	4

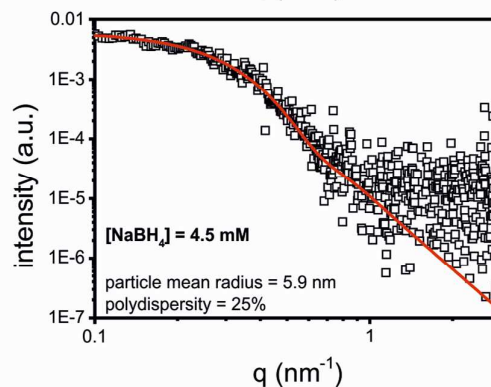
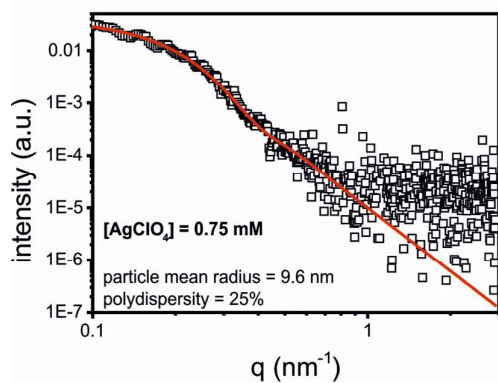
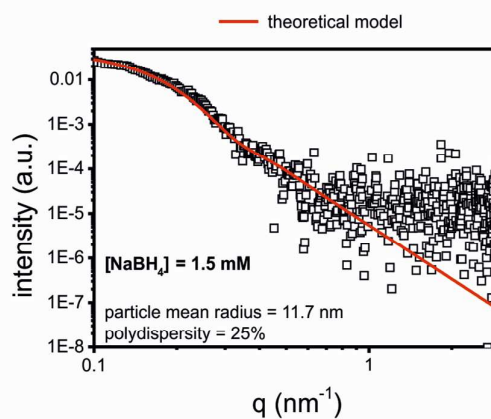
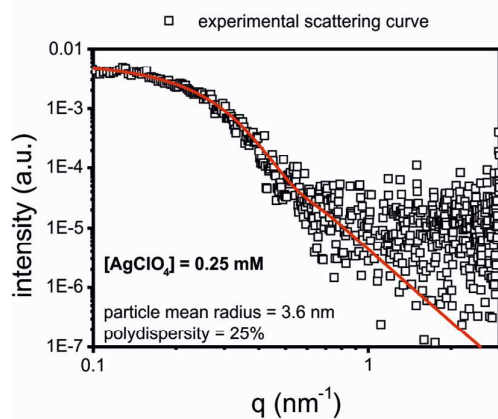
mean radius

### Variation of the $\text{NaBH}_4$ concentration for $[\text{AgClO}_4] = 0.5 \text{ mM}$

b)	$[\text{NaBH}_4]$	1.5 mM	2.25 mM	3 mM	3.75 mM	4.5 mM
	mean radius	11.4 nm	10.6 nm	9.9 nm	8.3 nm	6.9 nm
	deviation of mean radius	0.6 nm	1.0 nm	0.6 nm	1.0 nm	1.0 nm
	duration of metastable state	74 sec	223 sec	437 sec	486 sec	903 sec
	$[\text{NaBH}_4]/[\text{AgClO}_4]$	2	4	6	8	12

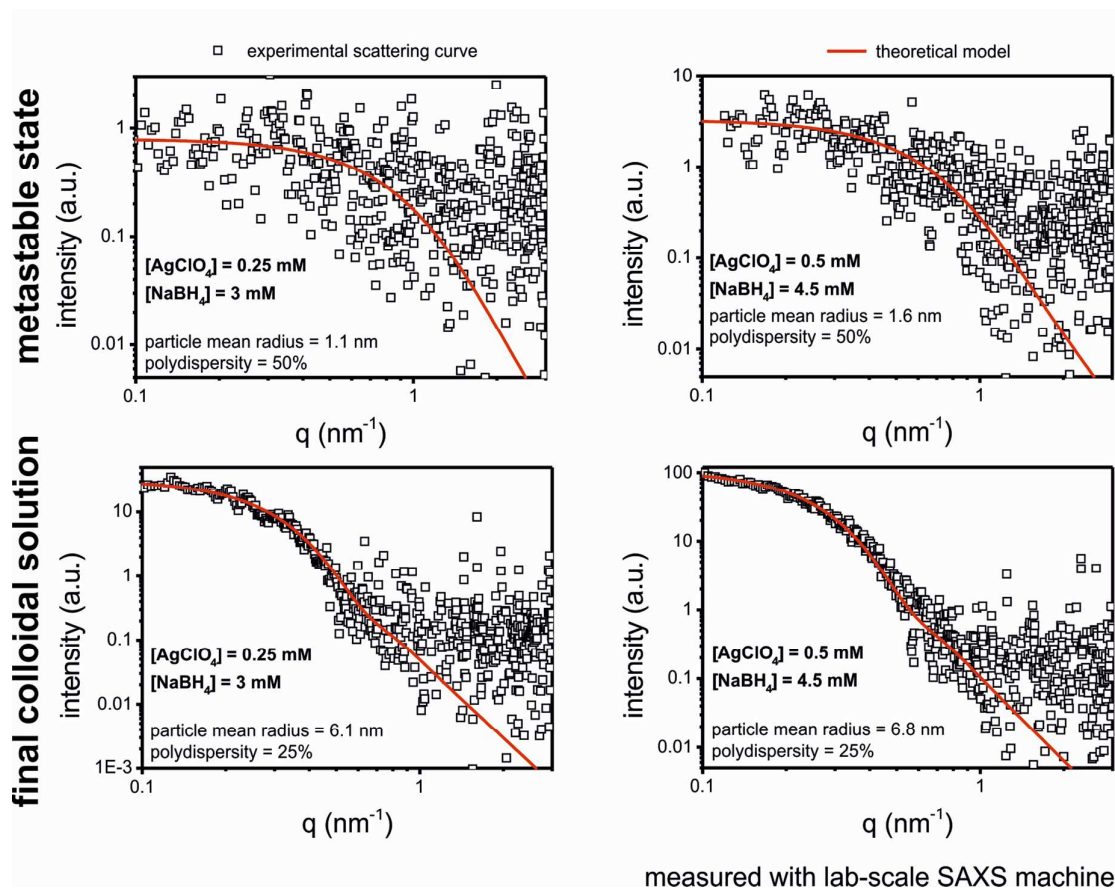
mean radius

SAXS data from variation of the  $\text{AgClO}_4$  and  $\text{NaBH}_4$  concentrations: selected scattering curves and the corresponding fits.



measured with lab-scale SAXS machine

SAXS data from time-resolved investigations of the growth mechanism with varied reactant concentrations: selected scattering curves and corresponding fits from the metastable phase and the final colloidal solution.

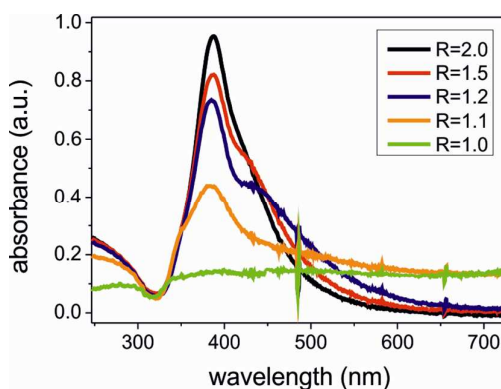


# SI-9

The table shows the results of SAXS investigations of final colloidal solutions which were synthesized using a 0.5 mM  $\text{AgClO}_4$  solution. The concentrations of the  $\text{NaBH}_4$  solutions are  $[\text{NaBH}_4] = R \cdot 0.5$  mM. The polydispersity is 30 %. The duration of the metastable state refers to the observed reaction time at which color change from yellow to brown occurs.

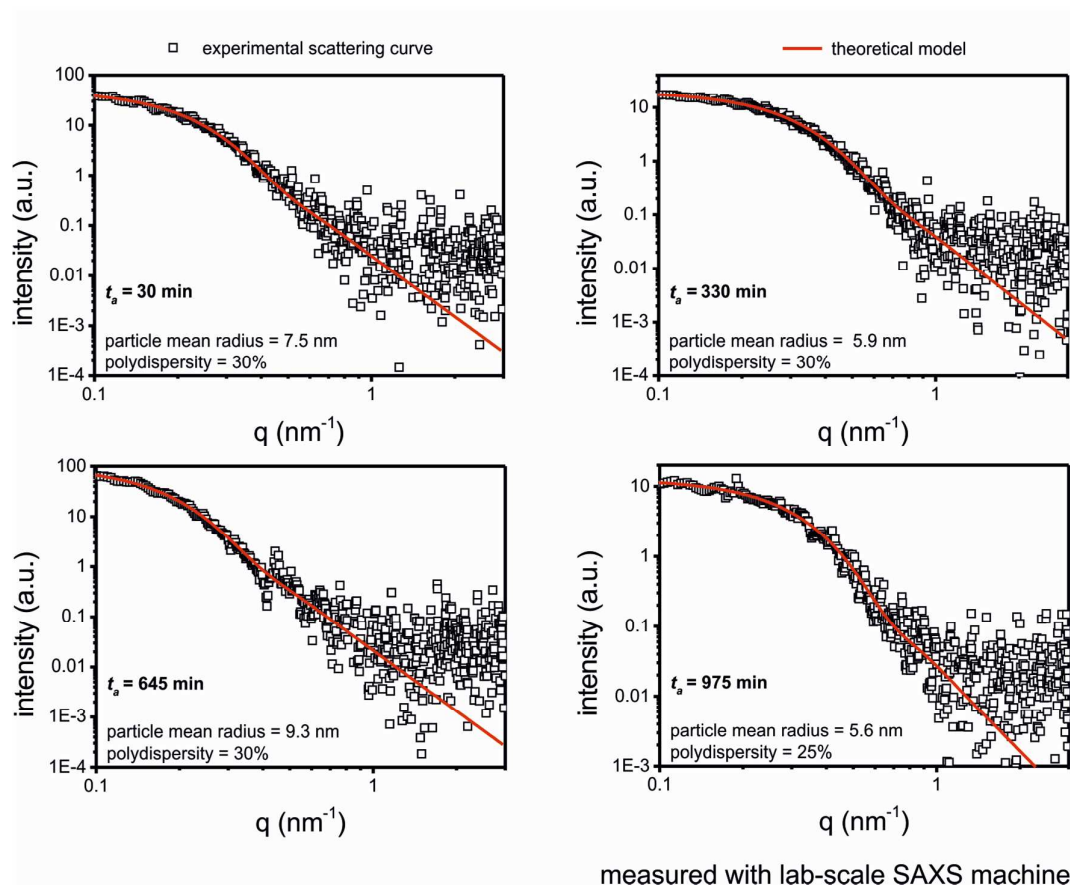
R	Final particle mean radius (nm)	Duration of metastable state (s)
2	6.9	30
	6.3	30
	6.3	40
1.5	7.4	7
	6.3	8
	7.2	7
1.2	9.2	5
	8.6	5
	9.2	5
1.1	10.9	2
	12.0	2
	11.4	1
1.0	Precipitation	0

The figure below displays UV-vis spectra of selected colloidal solutions. The main peak at approx. 385 nm decreases with decreasing R (excess of  $\text{NaBH}_4$ ). The broadening of the plasmon resonance can be ascribed to the formation of large aggregates. For  $R=1.0$ , the particles precipitate within a short time. Thus, no plasmon resonance is observed.



# SI-10

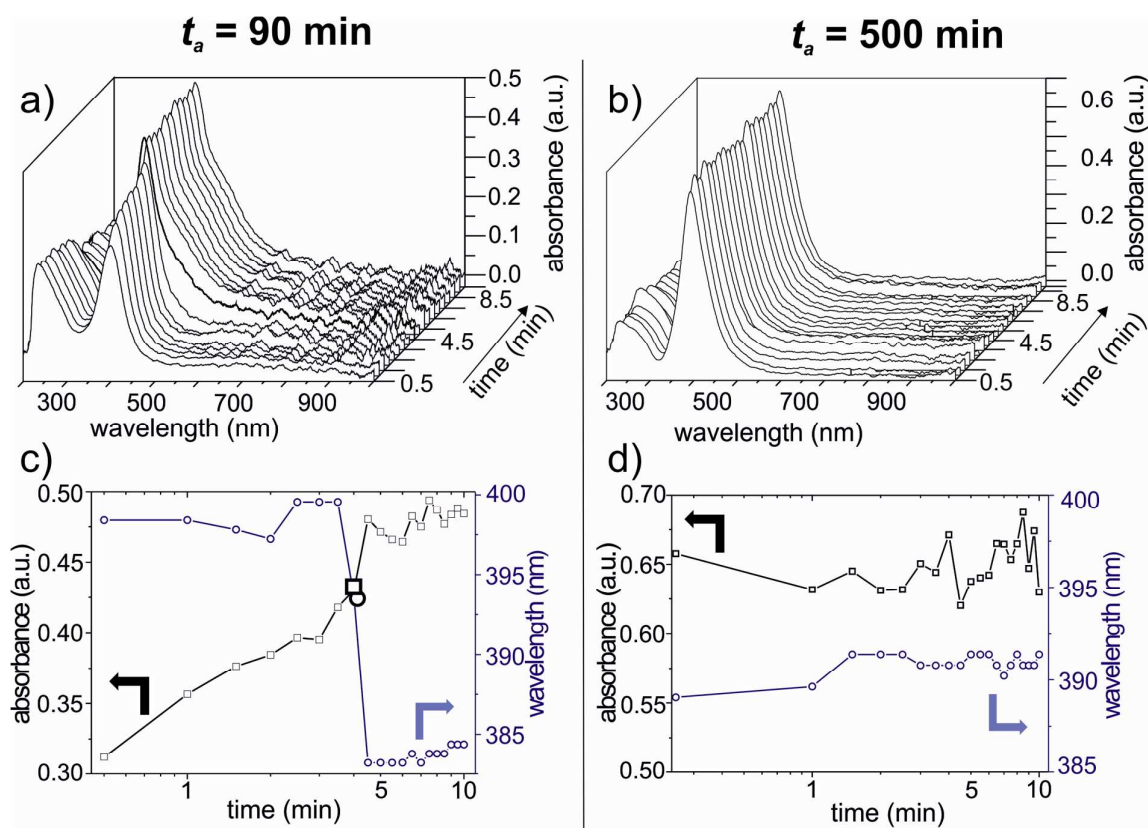
SAXS data from the investigation of the influence of  $\text{NaBH}_4$  aging time  $t_a$  on the final size distribution: selected scattering curves and corresponding fits for different  $t_a$ .



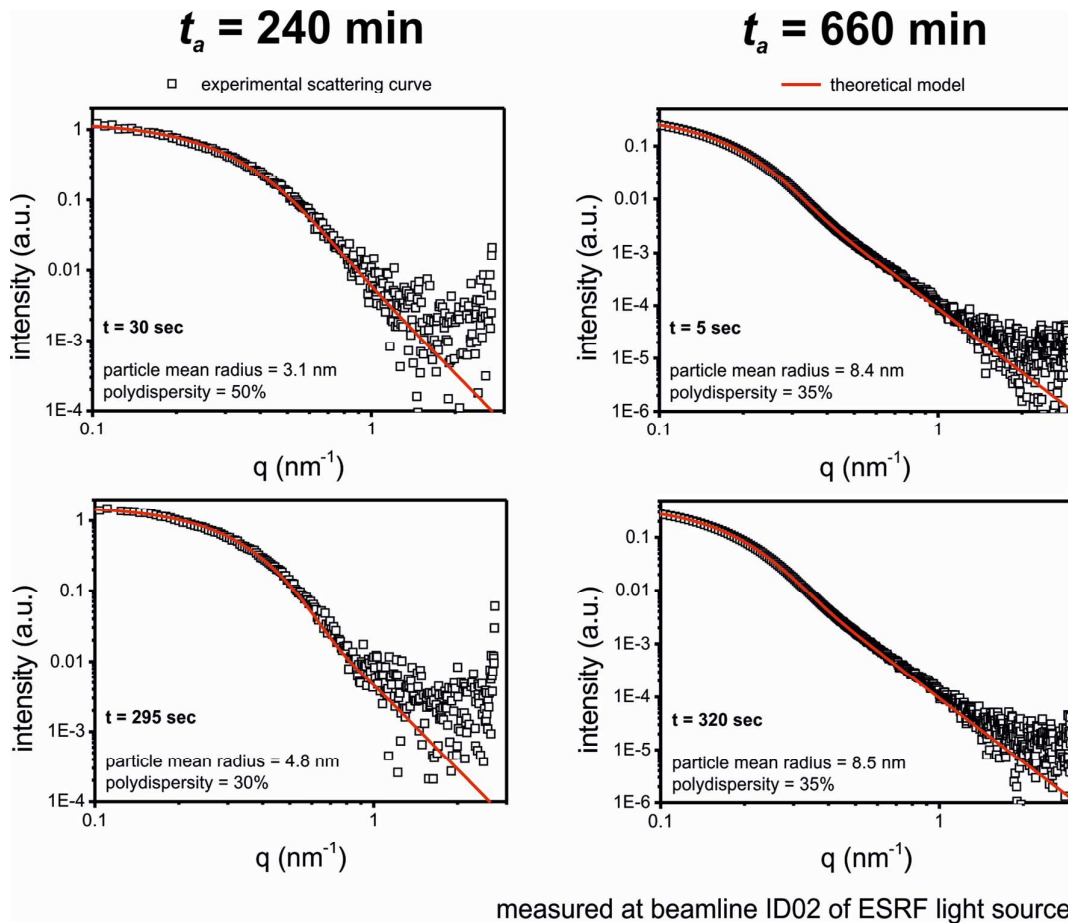
The figure below shows the results of time-resolved UV-vis investigations using aged reducing agent solution to synthesize the colloidal solution. a) UV-vis spectra vs. time for an aging time  $t_a = 90$  min, b) UV-vis spectra vs. time for  $t_a = 500$  min, c) absorbance and wavelength of maximum absorbance vs. time for  $t_a = 90$  min, d) absorbance and wavelength of maximum absorbance vs. time for  $t_a = 500$  min.

For  $t_a = 90$  min, the wavelength of the main peak shifts from 397 nm to 384 nm at approx. 240 sec which indicates the end of the metastable state.

For  $t_a = 500$  min, the spectrum remains constant (first available curve at  $t = 15$  sec) with a maximum absorbance at 390 nm. The results do not indicate a metastable state.



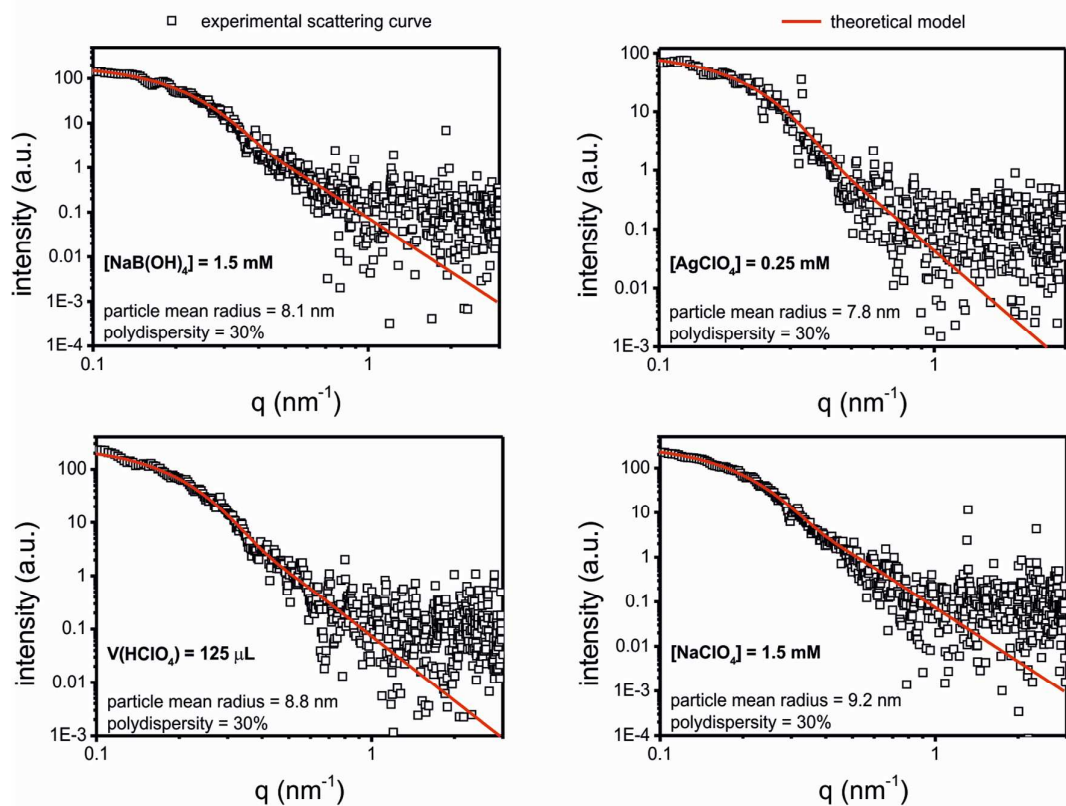
SAXS data from the time-resolved investigation of the influence of  $\text{NaBH}_4$  aging time  $t_a$  on the particle growth mechanism: selected scattering curves and corresponding fits for different  $t_a$  and reaction times.





# SI-13

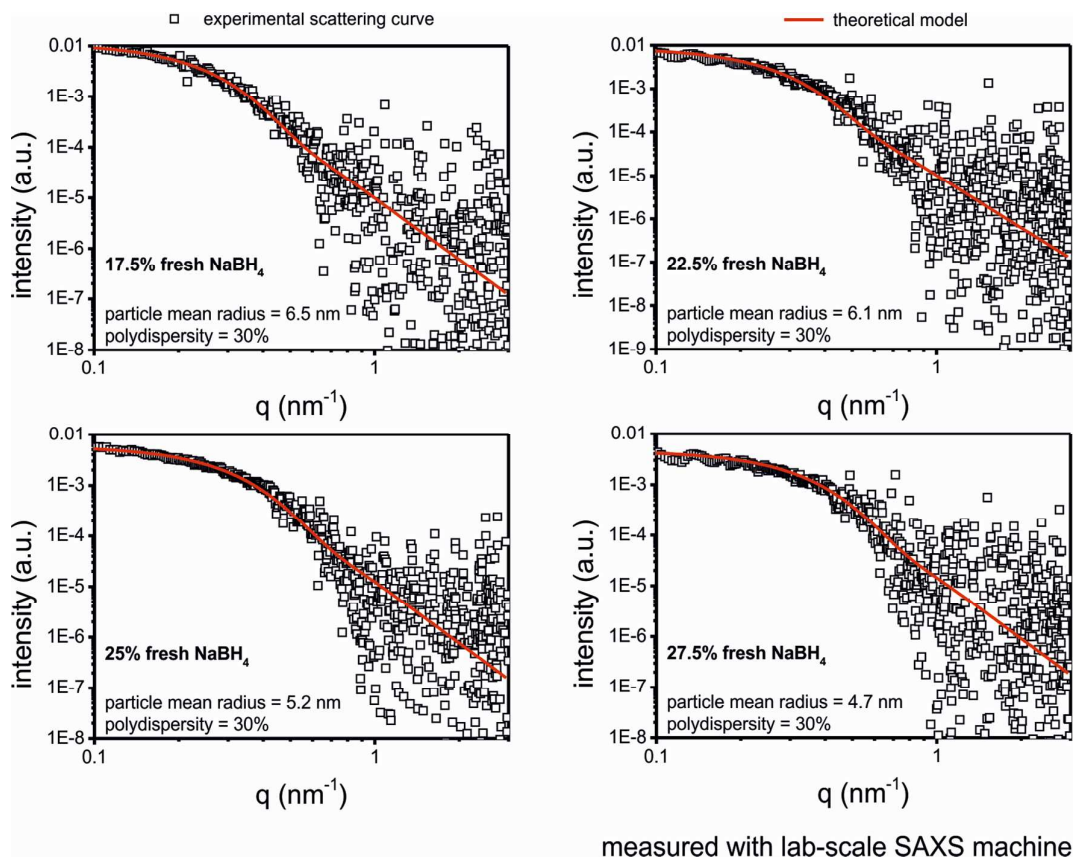
SAXS data from parameter variation study within the plateau: selected scattering curves and corresponding fits.



measured with lab-scale SAXS machine



SAXS data from variation of the reducing agent solution (mixing fresh and aged  $\text{NaBH}_4$ ): selected scattering curves and corresponding fits.



## References

- (1) Glavée, G. N.; Klabunde, K. J.; Sorensen, C. M.; Hadjipanayis, G. C. *Langmuir* **1994**, *10*, 4726–4730.
- (2) Edwards, J. O.; Morrison, G. C.; Ross, V. F.; Schultz, J. W. *J. Am. Chem. Soc.* **1955**, *77*, 266–268.
- (3) Soler, L.; Macanás, J.; Muñoz, M.; Casado, J. *International Journal of Hydrogen Energy* **2007**, *32*, 4702–4710.
- (4) Andrieux, J.; Demirci, U. B.; Hannauer, J.; Gervais, C.; Goutaudier, C.; Miele, P. *International Journal of Hydrogen Energy* **2011**, *36*, 224–233.
- (5) Dai, H.-B.; Ma, G.-L.; Kang, X.-D.; Wang, P. *Catalysis Today* **2011**, *170*, 50–55.
- (6) Churikov, A. V.; Gamayunova, I. M.; Zapsis, K. V.; Churikov, M. A.; Ivanishchev, A. V. *International Journal of Hydrogen Energy* **2012**, *37*, 335–344.
- (7) Gonçalves, A.; Castro, P.; Novais, A.; Fernandes, V. R.; Rangel, C. M.; Matos, H. *Reactions* **2007**, *1*, 2.
- (8) Sun, Y.; Xia, Y. *Science* **2002**, *298*, 2176–2179.
- (9) Polte, J.; Tuae, X.; Wuithschick, M.; Fischer, A.; Thuenemann, A. F.; Rademann, K.; Kraehnert, R.; Emmerling, F. *ACS Nano* **2012**, *6*, 5791–5802.